

Anomalous low-energy properties in amorphous solids and the interplay of electric and elastic interactions of tunneling two-level systems

Alexander Churkin,^{1,2} Shlomi Matityahu,^{2,3,4} Andrii O. Maksymov,⁵ Alexander L. Burin,⁵ and Moshe Schechter²

¹*Department of Software Engineering, Sami Shamoon College of Engineering, Beer-Sheva, Israel*

²*Department of Physics, Ben-Gurion University of the Negev, Beer Sheva 84105, Israel*

³*Institute of Nanotechnology, Karlsruhe Institute of Technology, D-76344 Eggenstein-Leopoldshafen, Germany*

⁴*Department of Physics, NRCN, P.O. Box 9001, Beer-Sheva 84190, Israel*

⁵*Department of Chemistry, Tulane University, New Orleans, LA 70118, USA*

(Dated: February 21, 2020)

Tunneling two-level systems (TLSs), generic to amorphous solids, dictate the low-energy properties of amorphous solids and dominate noise and decoherence in quantum nano-devices. The properties of the TLSs are generally described by the phenomenological standard tunneling model. Yet, significant deviations from the predictions of this model found experimentally suggest the need for a more precise model in describing the low-energy properties of amorphous solids. Here we show that the temperature dependence of the sound velocity, dielectric constant, specific heat, and thermal conductivity, can be explained using an energy-dependent TLS density of states. The reduction of the TLS density of states at low energies relates to the ratio between the strengths of the TLS-TLS interactions and the random potential, which is enhanced in systems with dominant electric dipolar interactions.

I. INTRODUCTION

Understanding the low-temperature physics of disordered and amorphous materials has emerged as one of the most intriguing and challenging problems in condensed matter physics [1, 2]. Below about 1 K, such systems exhibit physical properties that are not only qualitatively different from those of crystalline solids, but also show a remarkable degree of universality [2–5]. For instance, the specific heat and thermal conductivity are approximately linear and quadratic in temperature, respectively, while the internal friction Q^{-1} is nearly temperature-independent and varies slightly between different materials.

This behavior of amorphous solids has been primarily interpreted with the model of tunneling two level systems (TLSs) [6, 7], suggesting the presence of atoms or groups of atoms tunneling between two nearly degenerate configurations, which will be referred to as the standard tunneling model (STM). There were numerous suggestions targeted to describe the nature of tunneling systems and their universality, including the soft-potential model [8] and its further developments (see Ref. 9 and references therein), interaction-based models targeted to account for quantitative universality of TLSs [1, 10–13], glass-transition-based theory [14, 15] and models based on the polaron effect [16, 17]. Similarly to the STM, all these theories account for the existence of TLSs at low temperatures and the resulting thermodynamic and acoustic properties of glasses. Yet, their predictive value lies in their deviations from the STM, which has to be checked against experimental observations [18].

Marked examples of discrepancies between experimental results and theoretical predictions of the STM are the deviations from integer powers of the temperature dependence of the specific heat and thermal conductivity, see

below, and the anomalous temperature dependence of the sound velocity and dielectric constant. The STM predicts logarithmic temperature dependence, with a maximum for the sound velocity and a minimum for the dielectric constant, with a slope ratio of 1 : -0.5 between the slopes below and above the crossover temperature. Yet, experiments find different value for this ratio of slopes, typically 1 : -1 [19–23].

Whereas the original formulation of the STM neglects interactions between the TLSs, it became apparent that interactions play a significant role in phenomena such as spectral diffusion and phonon echoes [12, 24, 25]. TLS-TLS interactions lead to a reduction of the TLSs density of states (DOS) near zero energy [12, 26, 27]. This reduction of the DOS scales with the ratio of the interaction strength to the disorder energy [13, 28–30], usually assumed to be much smaller than unity.

At the same time, there is a growing body of evidence for an energy-dependent DOS at low energies, of the form $n(E) \propto E^\mu$, with $0.1 < \mu < 0.3$. Even stronger energy dependence of the DOS in a-SiO was recently extracted from measurements of dielectric loss using superconducting lumped element resonators [31]. These findings are supported by earlier experiments which show indirect evidences for energy-dependent DOS: in deviations from STM predicted integer values for the temperature dependence of the specific heat, $C \propto T^{1+\alpha}$, and of the thermal conductivity, $\kappa \propto T^{2-\beta}$, with $\alpha, \beta \approx 0.1 - 0.3$ [4, 32, 33]; and in the linewidth of optical transitions of ions and molecules embedded in glasses having an unusual temperature dependence $\propto T^{1.3}$ [34–36], which may arise due to dipolar interactions between the TLSs, assuming a DOS $n(E) \propto E^\mu$, with $\mu \approx 0.3$ [37–39]. In addition, a DOS $n(E) \propto E^\mu$ with $\mu \approx 0.3$ was recently assumed in Refs. [40–42] in an effort to provide a theoretical explanation to the temperature and power dependence of $1/f$ noise in superconducting resonators at low temperatures

(see, however, Ref. 43). Still, it is not clear what the origin of such marked energy dependence of the TLS-DOS may be.

Here we calculate the single-particle TLS-DOS assuming TLS disorder energy being not much larger than the TLS-TLS interaction energy. At zero temperature we find the TLS-DOS to be significantly reduced, and well-described by a power law, the power being approximately the ratio between interaction and disorder. Since the single-particle TLS-DOS involves the excitation energies of single TLSs in the environment of all other TLSs, it is temperature dependent. Indeed, at finite temperature the pseudo-gap at low energies closes gradually.

Intriguingly, we find that energy-dependent TLS-DOS accounts well not only for the anomalous power laws of the temperature dependence of the specific heat and thermal conductivity, but also for the anomalous temperature dependence of the sound velocity and dielectric constant. We discuss the energy dependence of the TLS-DOS within the Dipolar Gap model [29] and the Two-TLS model [13]. Using the latter model we show that TLS-TLS interactions not much smaller than the random fields arise once TLS-TLS interactions are dominated by the electric dipolar interaction. Relation to existing experimental results is then discussed.

The paper is organized as follows: In Sec. II we introduce the generic model for TLSs, albeit allowing for arbitrary ratio between the typical TLS-TLS interactions at short distances and the typical random field. We then discuss the relation between this model and the Dipolar Gap model. In Sec. III we first present (Sec. III A) the numerical results for the single-particle TLS-DOS for different ratios of interactions to random fields, and the resulting temperature dependence of the thermal conductivity and specific heat (Sec. III B). We then address (Sec. III C) the anomalous temperature dependence of the sound velocity and dielectric constant, within the Dipolar Gap model, and within the model allowing for stronger TLS-TLS interactions. In Sec. IV we discuss, within the Two-TLS model, the possibility of TLS-TLS interactions enhancement as a result of dominance of electric interactions over elastic interactions in amorphous solids. We then summarize in Sec. V.

II. MODEL AND TLS-DOS

At low energies the system of interacting TLSs can be modelled by the effective Hamiltonian [6, 7, 11, 24]

$$\mathcal{H}_{\text{TLS}} = \sum_i h_i \tau_i^z + \sum_i \Delta_{0,i} \tau_i^x + \frac{1}{2} \sum_{i \neq j} J_{ij} \tau_i^z \tau_j^z, \quad (1)$$

where τ_i^z and τ_i^x are the Pauli matrices that represent the TLS at site i . The first term is the bias energy of the TLSs resulting from their interaction with static disorder. The total bias energy of TLS i is therefore $\Delta_i \equiv h_i + \sum_j J_{ij} \tau_j^z$, and the total energy of a TLS is given by $E =$

$\sqrt{\Delta^2 + \Delta_0^2}$. Within the STM one assumes that $J_{ij} \ll h_i$, and that h_i are homogeneously distributed, leading to the ansatz $P(\Delta, \Delta_0) = P_0/\Delta_0$ and density of states $n = P_0 L_0$. Here $L_0 = \ln(\tilde{E}/\Delta_{0,\min})$, with \tilde{E} being a large energy of the order of the disorder energy and $\Delta_{0,\min}$ denoting the minimum tunneling amplitude of the TLSs. Generally, however, one allows energy dependence of the TLS-DOS, i.e. $n(E) = P_0(E) L_0$.

The second term in the Hamiltonian (1) denotes TLS tunneling. Whereas this term is of utmost importance to dynamic properties, it has a small effect on the TLS-DOS, especially at energies $\gtrsim 10$ mK relevant to most experiments. We therefore consider henceforth the random-field Ising Hamiltonian

$$\mathcal{H} = \sum_i h_i \tau_i^z + \frac{1}{2} \sum_{i \neq j} J_{ij} \tau_i^z \tau_j^z, \quad (2)$$

with $h_i = h_0 c_i$ and $J_{ij} = c_{ij} J_0 / (R_{ij}^3 / R_0^3 + C)$, where c_i and c_{ij} are normally distributed random variables with zero mean and unity variance, R_{ij} is the distance between TLS i and TLS j , R_0 is the typical distance between nearest TLSs, J_0 denotes typical nearest neighbor TLS-TLS interaction, C is a short distance cutoff, and h_0 is the typical random field. Generally, the interaction term comprises both elastic and electric TLS-TLS interactions.

Adding weak interactions to the STM, i.e. considering $J_0/h_0 \ll 1$, and assuming $T = 0$, one finds the emergence of a dipolar gap at low energies [11, 24, 29]

$$n(E) = \frac{n_0}{1 + c \tilde{J}_0 n_0 \cdot \log(\tilde{J}_0 / R_0^3 E)}, \quad (3)$$

where $c = 2\pi/3$, $\tilde{J}_0 \equiv J_0 R_0^3$ is the interaction constant, and $n_0 \equiv n(E = J_0) = 1/(h_0 R_0^3)$. Widespread experimental evidence for the low-temperature universality of acoustic properties in amorphous solids dictate, for the elastic interactions, a value of $J_0/h_0 = \tilde{J}_0 n_0 \approx 0.03 - 0.05$ [6, 7]. Below we discuss the energy-dependent TLS-DOS and its consequences within the dipolar gap model, and within a model of the Hamiltonian (2), taking, however, J_0/h_0 to be not much smaller than unity - possible reason may be domination of electric dipolar interactions.

III. RESULTS

A. TLS-DOS

We now calculate the TLS-DOS within the model presented by the Hamiltonian (2) with $J_0/h_0 = 0.2, 0.3$. To demonstrate the power-law-like energy dependence of the low-energy TLS-DOS we perform Monte Carlo simulations on cubic lattices of size L^3 , with $L = 8, 12$, and periodic boundary conditions are imposed. TLSs are placed randomly in the lattice with concentration $x = 0.5$, and

we choose $h_0 = 10$ K in accordance with its calculated value for KBr:CN [44]. We note that the choice of lattice structure is for convenience, and the randomness of TLS positions in the amorphous solids is retained by the random dilution and by the randomness in c_i and c_{ij} . We further note that the lattice constant R_0 denotes typical distance between adjacent TLSs, rather than interatomic spacing. We use a short distance cutoff equal to R_0 (i.e. $C = 1$) to account for the finite size of the TLSs, but decreasing the value of the cutoff has minimal effect on our results.

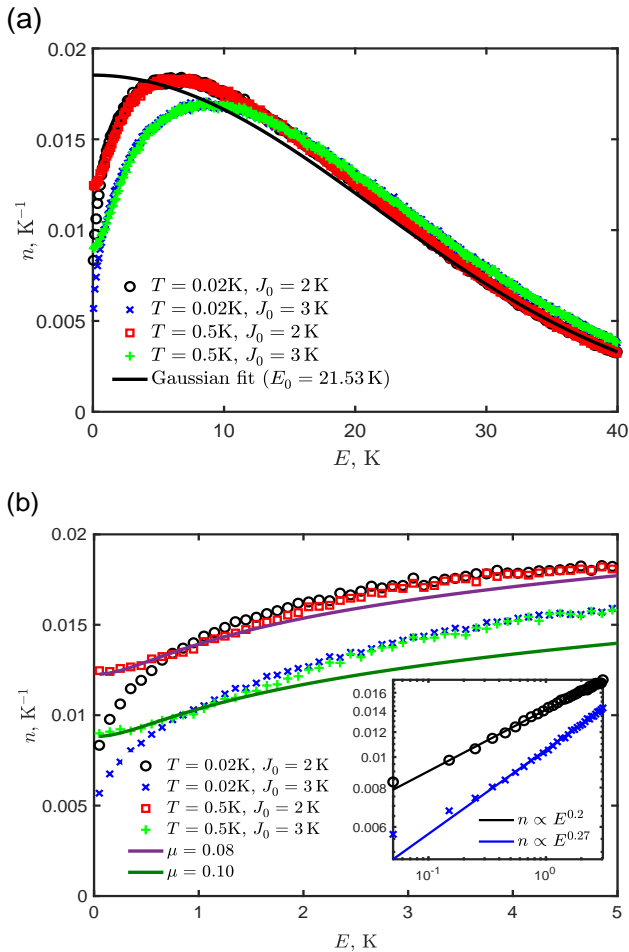


FIG. 1. (Color online) (a) Single-particle TLS-DOS at $T = 0.02, 0.5$ K, obtained by simulated annealing MC simulations with $L = 12$ and $J_0 = 2, 3$ K ($J_0/h_0 = 0.2, 0.3$). Gaussian fit (solid black) to the data at $J_0 = 2$ K, corresponding to the limit of negligible TLS-TLS interactions. (b) Zoom in to low energies. Solid lines describe low-energy fits, using Eq. (4), for the curves corresponding to $T = 0.5$ K. Inset shows fits to the form $n \propto E^\mu$ for the curves corresponding to $T = 0.02$ K. Note that the power μ decreases with increasing temperature.

Simulated annealing MC simulations are performed at 42 temperatures decreasing from 300 K to 0.02 K, and then at $2 \mu\text{K}$ to emulate zero temperature, and are used to calculate the single-particle DOS, $n(T, E)$. While the

system does not fully equilibrate within the simulated annealing technique, we verify that the final state at $2 \mu\text{K}$ is stable against single and double spin flips. This constitutes the sufficient condition for the determination of the DOS given by the Efros-Shklovskii stability criterion [26, 27]. The single-particle DOS at a given temperature is then calculated by measuring the excitation energies of single TLSs in a given realization, and averaging over 10^4 independent disorder realizations.

In Fig. 1 we plot $n(T, E)$ as a function of energy for $T = 0.02$ K and $T = 0.5$ K, interaction strengths $J_0 = 2, 3$ K, and lattice size $L = 12$. In the absence of interactions, the DOS is well-described by a Gaussian [solid black curve in Fig. 1(a)] with width of order $h_0 = 10$ K [13, 30]. The dipolar interactions produce an Efros-Shklovskii type pseudo-gap for energies below $\sim J_0$ [26, 27, 29]. As $T \rightarrow 0$, the DOS at low energies approaches a form well-described by power law energy dependence, $n(T \rightarrow 0, E) \propto E^\mu$, with $\mu \approx 0.2 - 0.3$ [the exact value of μ depends on J_0 , see inset of Fig. 1(b)]. The dipolar gap is suppressed as the temperature increases, yielding a DOS which at low energies is rather well-approximated by the function

$$n(T, E) \approx B(T)(T^2 + E^2)^{\mu(T)/2}. \quad (4)$$

We note that the pseudo-gap closes at finite temperature and therefore the power $\mu(T)$ decreases with increasing temperature.

B. Thermal conductivity and specific heat

Being well-approximated with a power law DOS at low energies, we expect the TLS-DOS calculated from the Hamiltonian (2) and plotted in Fig. 1 to account well for the deviations from integer power law exponents of the temperature dependences of the thermal conductivity and specific heat as observed in amorphous solids. Having calculated $n(T, E)$, the thermal conductivity $\kappa(T)$ is found by calculating [5]

$$\kappa(T) = \frac{1}{3} \sum_{\alpha} \int_0^{\infty} C_{\text{ph},\alpha}(E) v_{\alpha} \ell_{\text{ph},\alpha}(E) dE \propto \int_0^{\infty} \frac{E^3 dE}{T^2 \sinh^2(E/2T) \tanh(E/2T) n(T, E)}, \quad (5)$$

where $C_{\text{ph},\alpha}(E) = E^4 / (8\pi^2 \hbar^2 v_{\alpha}^3 T^2 \sinh^2(E/2T))$ is the Debye heat capacity for phonons at a given energy E and polarization α , v_{α} is the sound velocity and $\ell_{\text{ph},\alpha}^{-1}(E) = (\pi \gamma_{\alpha}^2 E / \rho v_{\alpha}^3) P_0(T, E) \tanh(E/2T) \propto (\pi \gamma_{\alpha}^2 E / \rho v_{\alpha}^3) n(T, E) \tanh(E/2T)$ is the phonon inverse mean free path due to interaction with resonant TLSs (i.e., TLSs with energy splitting equal to the phonon energy), characterized by the coupling strength γ_{α} , and ρ denotes the mass density. The prefactor in Eq. (5) contains material-dependent constants which are indepen-

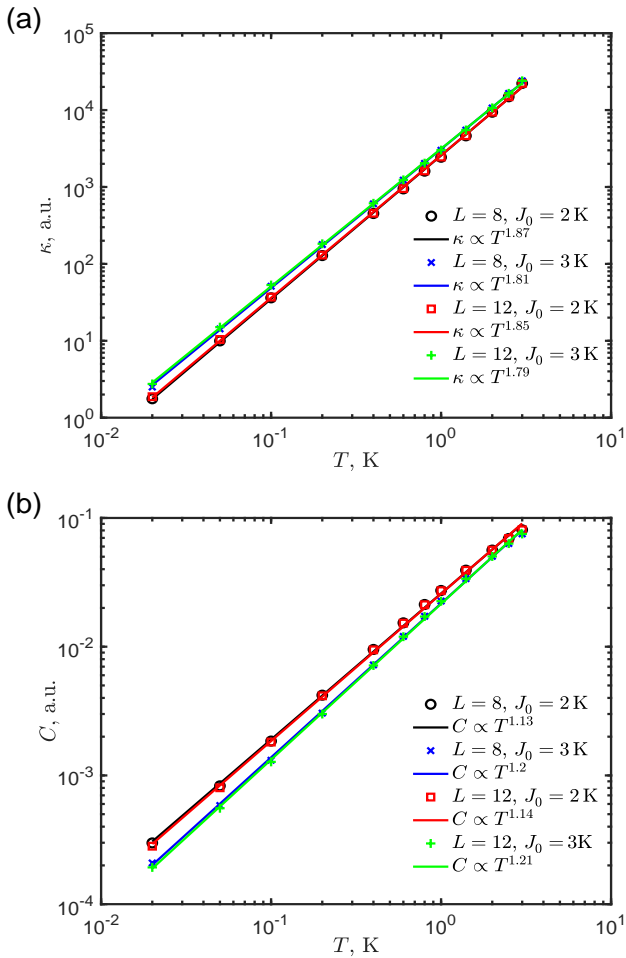


FIG. 2. (Color online) Temperature dependence of (a) Thermal conductivity (in arbitrary units) and (b) specific heat, obtained by Eqs. (5) and (6) with the TLS-DOS $n(T, E)$ computed by simulated annealing MC simulations with $L = 8, 12$ and $J_0 = 2, 3$ K (isolated points). Solid lines are fits to the form $\kappa \propto T^{2-\beta}$ and $C \propto T^{1+\alpha}$. Calculations correspond to a relaxed system close to equilibrium, see text.

dent of temperature. To study the temperature dependence of the thermal conductivity we calculate the last integral in Eq. (5), and represent the thermal conductivity in arbitrary units. Similarly, the specific heat $C(T)$ is evaluated, taking the Boltzmann constant $k_B = 1$, as [5]

$$C(T) = \int_0^\infty \frac{n(T, E) E^2 dE}{4T^2 \cosh^2(E/2T)}. \quad (6)$$

Figure 2 shows log-log plots of the thermal conductivity and the specific heat as a function of temperature, for $J_0 = 2, 3$ K and $L = 8, 12$. In all cases, the thermal conductivity and the specific heat obey a power law dependence, $\kappa \propto T^{2-\beta}$ and $C \propto T^{1+\alpha}$, with α and β in the range $0.1 - 0.2$. Note that we do not consider here the slow logarithmic time dependence of the specific heat, resulting from the large variance in TLS relaxation times, that can enhance the temperature dependence. Our re-

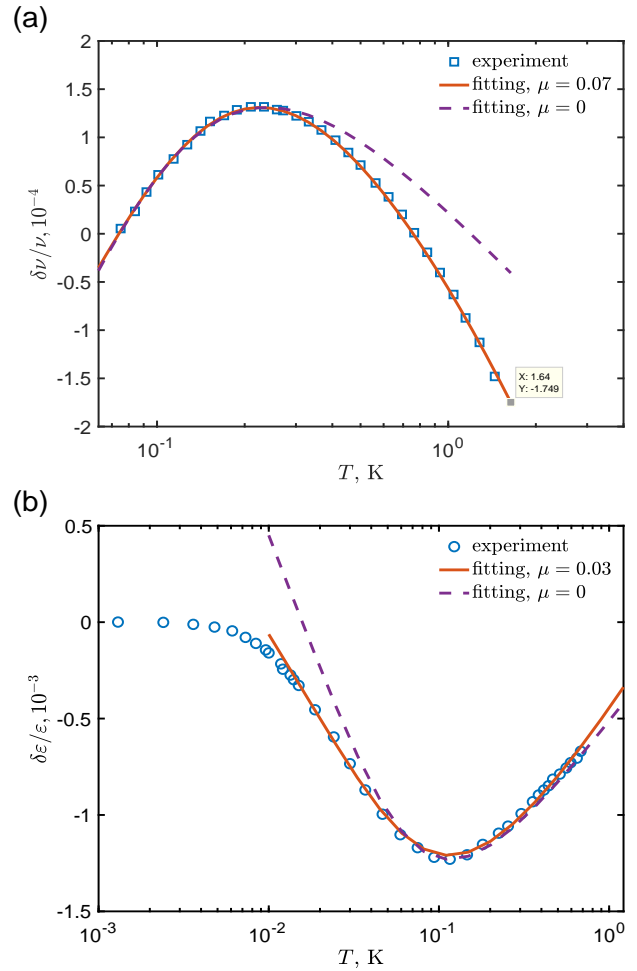


FIG. 3. (Color online) Temperature dependence of (a) sound velocity [23] and (b) dielectric constant of vitreous silica [22]. Solid lines correspond to fits by the sum of Eqs. (7) and (8), using for ω the experimental values [90KHz in (a), 1KHz in (b)], and using the fitting parameters A [9.4MHz in (a), 7.9MHz in (b)] and $P_0\gamma^2/\rho v^2$ [$3.2 \cdot 10^{-4}$ in (a), $8 \cdot 10^{-4}$ in (b)]. The DOS is taken from Eq. (4) using temperature independent finite $\mu > 0$ as a fitting parameter. Dashed lines are best fits with $\mu = 0$ as is given by the STM.

sults correspond to a given long time, as the system is out of equilibrium.

C. Sound velocity and dielectric constant

Given the above mentioned long-standing discrepancy between STM predictions and experimental results, it is of interest to study the consequences of energy-dependent TLS-DOS on the temperature dependence of the sound velocity and dielectric response at low temperatures. The temperature dependence of these quantities has two contributions coming from the resonant and relaxation processes [5]. Considering the sound velocity, the contribu-

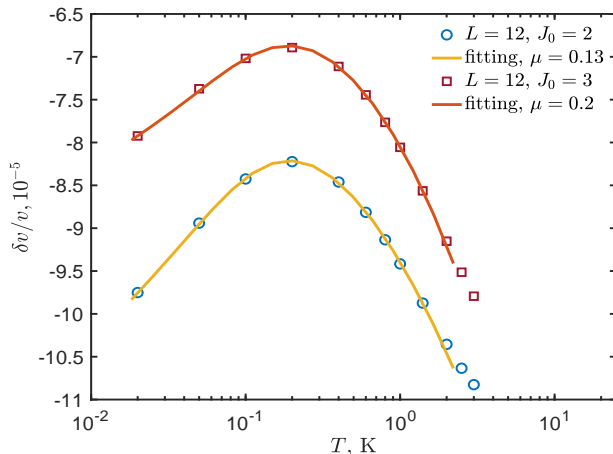


FIG. 4. (Color online) Temperature dependence of acoustic velocity, derived from the TLS-DOS obtained numerically from Eq. (2), for 12 different temperatures, for $L = 12$, $J_0 = 2$ (circles) and $J_0 = 3$ (squares). Solid lines are fits by the sum of Eqs. (7) and (8), using Eq. (4) for the TLS-DOS with temperature independent μ as a fitting parameter. Discrepancy between the power of the calculated energy-dependent DOS ($\mu = 0.2, 0.27$ for $J_0 = 2, 3$, respectively, see Fig. 1) and fit ($\mu = 0.13, 0.2$ for $J_0 = 2, 3$, respectively) is attributed to the temperature dependence of the power μ not taken into account in the fit using Eq. (4).

tion of the resonant process is of the form

$$\frac{\delta v_{\text{res}}}{v} = -\frac{1}{L_0} \frac{\gamma^2}{\rho v^2} \int_0^\infty \frac{n(T, E) dE}{E} \tanh\left(\frac{E}{2T}\right), \quad (7)$$

where v and γ are characteristic values for the velocity and for the interaction constant. For the relaxation process one has

$$\begin{aligned} \frac{\delta v_{\text{rel}}}{v} = & -\frac{1}{L_0} \frac{\gamma^2}{\rho v^2} \int_0^\infty \frac{n(T, E) dE}{2T \cosh^2(E/2T)} \\ & \times \int_0^1 \frac{\sqrt{1-x^2} dx}{x} \frac{1}{1 + \frac{\omega^2}{[Ax^2 E^3 \coth(E/2T)]^2}}, \quad (8) \end{aligned}$$

such that $\delta v/v = (\delta v_{\text{res}} + \delta v_{\text{rel}})/v$. Here ω is the probing frequency and $A \equiv \omega/T_0^3$, where T_0 is a crossover temperature of the order of the temperature at which the sound velocity obtains a maximum value [5]. The corresponding expressions for the dielectric constant ϵ are obtained by substituting $\gamma^2/(\rho v^2) \rightarrow p^2/(4\pi\epsilon_0)$, where p is the TLS dipole moment and ϵ_0 is the vacuum permittivity.

Fitting of experimental data for the temperature dependence of the sound velocity and dielectric constant requires a numerical calculation of the TLS-DOS $n(T, E)$ at many values of the ratio J_0/h_0 , which is a complicated task. We therefore take first a simpler approach and consider the dependence of the TLS-DOS on energy and temperature as given in Eq. (4), allowing the power μ to serve as a free fitting parameter independent of temperature. In Fig. 3 we show fits to typical experimental

data for sound velocity and dielectric response in amorphous solids at low temperatures. These data, displaying the usually found ratio of $1 : -1$ between the responses below and above the crossover temperature T_0 , are well fit by the sum of Eqs. (7) and (8), using the DOS $n(T, E)$ of Eq. (4) with a rather small power $\mu \approx 0.03-0.07$. Such a small power is consistent with the dipolar gap theory prediction for the energy dependence of the TLS-DOS, given by Eq. (3) [29].

To analyze the quality of the above fitting, we now compare it with the predictions of the full numerical simulation, using the above results for the numerically calculated $n(T, E)$ for the Hamiltonian 2 with ratios $J_0/h_0 = 0.2, 0.3$. In Fig. 4 we plot the sound velocity calculated as the sum of Eqs. (7) and (8), using the numerically calculated DOS for twelve temperatures below and above the temperature corresponding to the maximum in sound velocity. We find the ratio between the logarithmic slopes below and above the crossover temperature to be roughly $1 : -1$ for $J_0/h_0 = 0.2$, and even a steeper descent beyond the crossover temperature for $J_0/h_0 = 0.3$. We then find a rather good fit of the numerical data using Eq. (4) with a fixed (temperature-independent) power μ for the DOS in Eqs. (7) and (8). We note that the temperature-independent values obtained ($\mu = 0.13, 0.2$ for $J_0/h_0 = 0.2, 0.3$, respectively) are intermediate between the powers μ describing the numerically simulated TLS-DOS at $T = 0.02$ K ($\mu = 0.2, 0.27$ for $J_0/h_0 = 0.2, 0.3$, respectively) and the numerically simulated TLS-DOS at $T = 0.5$ K [$\mu = 0.08, 0.1$ for $J_0/h_0 = 0.2, 0.3$, respectively, see Fig. 1(b)].

Based on this analysis, one observes that the constant value of μ used to fit the numerical data in Fig. 4 underestimates the exponent of the energy dependence of the TLS-DOS at $T = 0$, and thus the value of J_0/h_0 . Accordingly, we expect that the $T = 0$ exponent describing the energy dependence of the TLS-DOS of the experimental system in Fig. 3 will be larger than the temperature-independent exponent $\mu \approx 0.03-0.07$ obtained in Fig. 3 using the approximate form of Eq. (4). Our numerical results therefore suggest that values of J_0/h_0 larger than those consistent with the dipolar gap theory of the STM may be needed to account for the temperature dependence of the sound velocity at low temperatures. As the dielectric constant differs from the sound velocity only by an overall prefactor, our results and conclusions above hold also for the anomalous temperature dependence of the dielectric constant.

IV. ELECTRIC DIPOLAR TLS-TLS INTERACTIONS

In Sec. III B we have discussed the effect of the interactions being not much smaller than the random field on the energy dependence of the TLS-DOS at low energies,

	Interaction between NN general defects	TLS disorder energy	Interaction between NN TLSs
Two-TLS model	$\sim \gamma_s^2/(\rho v^2 R_0^3) \sim T_g \approx 300 - 1000$ K	$h_0 \sim \gamma_s \gamma_w/(\rho v^2 R_0^3) \approx 10$ K	$J_0 \sim \gamma_w^2/(\rho v^2 R_0^3) \approx 0.1 - 0.3$ K
Two-TLS model with strong electric dipolar interactions	$\sim \gamma_s^2/(\rho v^2 R_0^3) \sim T_g \approx 300 - 1000$ K	$h_0 \sim \gamma_s \gamma_w/(\rho v^2 R_0^3) \approx 10$ K	$J_0 \sim p^2/(4\pi\epsilon\epsilon_0 R_0^3) \approx 2 - 3$ K

TABLE I. Comparison between: typical energy scales of the interactions between nearest neighbor (NN) defects; the resulting disorder energies for the abundant (τ)-TLSs at low energies, dominating low-temperature physics; and the interactions between (τ)-TLSs. (i) (top row) as derived by the Two-TLS model with dominant elastic interactions [13], (ii) (bottom row) as presented here for the Two-TLS model with strong electric dipolar interactions. Note the small TLS disorder energies in comparison to the value of 300 – 1000 K assumed by the STM.

and consequently on the anomalous power laws of the temperature dependence of the specific heat and thermal conductivity. In Sec. III C we have shown that such a J_0/h_0 ratio, larger than dictated by experimental results for the elastic interactions [1], may be needed to explain the temperature dependence of the sound velocity and the dielectric constant at low temperatures. In this section we discuss what may be a cause for an enlarged ratio of interaction strength to random field strength, and specifically the consequences of TLSs having larger electric dipolar interaction compared to their phonon-mediated interaction.

Amorphous solids show quantitative universality in their low-temperature acoustic properties. This universality suggests a small and universal value for the quantitatively universal product $P_0 \tilde{J}_0$, translating to a small and universal ratio between the elastic interaction and the random field. The emergence of a larger ratio of J_0/h_0 in the presence of dominant electric dipolar interactions is naturally obtained within the theoretical framework of the Two-TLS model [13]. We thus begin with a presentation of the main features of the Two-TLS model relevant to our discussion. A more detailed discussion of the model is deferred to Appendix A.

First considering only elastic interactions, the Two-TLS model divides TLSs into two groups, with bimodal distribution of their interaction strengths with the strain, denoted by γ_w for the weakly interacting τ -TLSs, which correspond to the abundant TLSs at low energies, and by γ_s for the other defects, where $g \equiv \gamma_w/\gamma_s \approx 0.02$ [13, 44–48]. The Hamiltonian 2 is then derived as the low-energy effective Hamiltonian of the system (see Ref. [13] and also App. A), with

$$h_i \approx \frac{c_i \gamma_w \gamma_s}{\rho v^2 R_0^3} \quad ; \quad J_{ij} \approx \frac{c_{ij} \gamma_w^2}{\rho v^2 R_{ij}^3}. \quad (9)$$

Here, R_0 is the typical distance between nearest two-level defects, R_{ij} denotes the distance between τ -TLS i and τ -TLS j , and the parameters $c_i, c_{ij} \sim O(1)$ can be regarded as normally distributed random variables [45].

The form of the Hamiltonian (2) is equivalent to that of the STM Hamiltonian, albeit within the Two-TLS model one can derive the typical magnitude of the interactions between the weakly interacting TLSs, as well as the typical magnitude of the random field. Since

typical disorder energy at nearest neighbor distance is $\approx \gamma_s^2/(\rho v^2 R_0^3) \sim T_g$, where $T_g \approx 300 - 1000$ K is the glass transition temperature, one finds that the typical disorder energy for a τ -TLS, which is g times smaller, is given by $h_0 \approx 10$ K [13, 30, 44, 47], and that TLS-TLS interactions at nearest neighbor distance have a typical value of $J_0 \approx gh_0 \approx 0.3$ K $\ll h_0$ [13, 30, 47].

Consider now the electric dipolar interaction,

$$J_{ij} \approx \frac{c_{ij} p^2}{4\pi\epsilon\epsilon_0 R_{ij}^3}. \quad (10)$$

The above characteristics of the TLSs within the Two-TLS model, including the relative smallness of the random fields, and the extreme smallness of the elastic TLS-TLS interaction, allow for the possibility of electric dipole interactions to dominate over the elastic TLS-TLS interactions, and to be not much smaller than the typical bias energies of the TLSs, i.e. $J_0/h_0 \lesssim 1$.

Experimentally, the ratio between the electric and elastic interactions can be deduced from combined measurements of dielectric loss and acoustic loss on the same material. Such measurements were carried out for BK7 and coverglass [49], indicating somewhat larger electric than elastic TLS-TLS interactions (see detailed analysis in Appendix B). Typical values of $\gamma_w \approx 1 - 2$ eV [50–53] and $p \approx 3 - 6$ D [53–58], and the corresponding parameters (mass density, sound velocity and dielectric constant) of selected amorphous solids (and specifically for amorphous solids relevant to modern superconducting qubits and microresonators, such as Al_2O_3 and Si_3N_4 [59]), suggest that larger values of $J_0^{\text{electric}}/J_0^{\text{elastic}} = (p^2 \rho v^2)/(4\pi\gamma^2 \epsilon\epsilon_0)$ may be expected.

In table I we summarize the typical energy scales of (a) interactions between general defects, which is of the order of the glass transition, and; (b) disorder energy and (c) typical TLS-TLS interaction energy - for the abundant (τ)-TLSs at low temperatures. All energy scales are denoted within the Two-TLS model with: (i) dominant elastic TLS-TLS interactions, and (ii) strong electric dipolar TLS-TLS interactions.

The relation suggested above between the magnitude of the power of the energy dependence of the TLS-DOS and the dominance of the electric dipolar interaction over the elastic interaction can be further examined by considering disordered lattices, where the TLS concentration

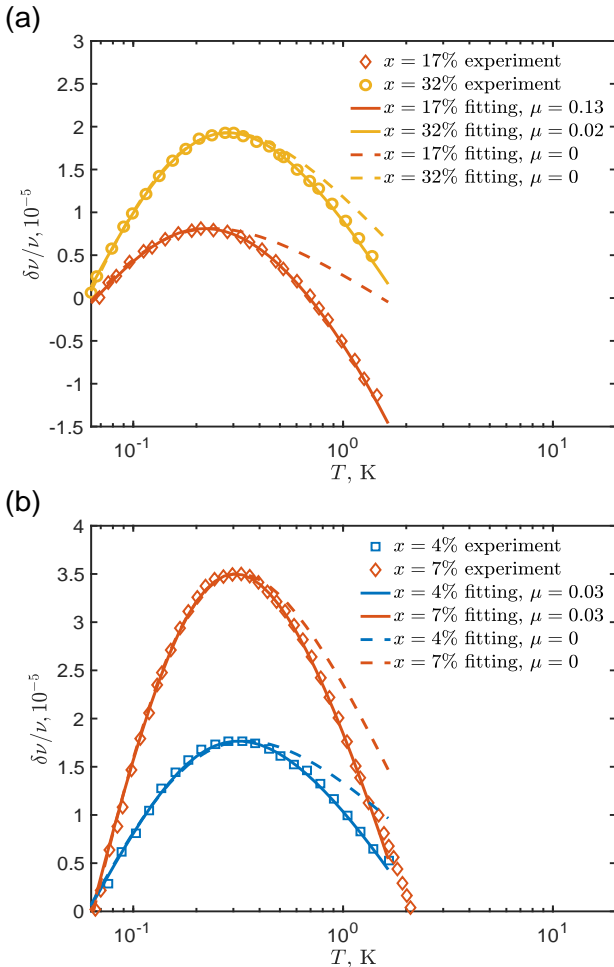


FIG. 5. (Color online) Temperature dependence of acoustic velocity. Points denote experimentally obtained values, taken at $\omega = 90\text{KHz}$ [23]. Solid lines correspond to fits by the sum of Eqs. (7) and (8), using Eq. (4) for the DOS with finite $\mu > 0$ as a fitting parameter. Dashed lines are best fits within the STM, i.e. with $\mu = 0$. (a) For $(\text{SrF}_2)_{1-x}(\text{LaF}_3)_x$. Here as x is enhanced so does the strain, and consequently the ratio of dipolar interaction to elastic interaction is decreased. Reduction of the power μ is in agreement with theory. Parameters used for best fits are $P_0\gamma^2/\rho v^2 = 1.9 \cdot 10^{-5}, 2.5 \cdot 10^{-5}$ and $A = 7.9\text{MHz}, 4.6\text{MHz}$, for $x = 0.17, 0.32$ respectively. (b) For $((\text{BaF}_2)_{0.5}(\text{SrF}_2)_{0.5})_{1-x}(\text{LaF}_3)_x$. Here the strain, and thus the ratio of electric to elastic interactions, are independent of x . Independence of the power μ on x is in agreement with theory. Parameters used for best fits are $P_0\gamma^2/\rho v^2 = 2.1 \cdot 10^{-5}, 4.5 \cdot 10^{-5}$ and $A = 3.5\text{MHz}, 3.9\text{MHz}$, for $x = 0.04, 0.07$ respectively.

can be varied [60]. Two protocols exist for the variation of the concentration of TLSs [23, 61]. In the first, TLSs are the sole defects in the lattice. In this case, increasing TLS concentration increases the strain in the system, and thus the coupling of τ -TLSs to the phonon field [13, 45]. In the second, TLS concentration is varied in a mixed lattice, in which strain is large already in the absence of TLSs. Thus, in the second protocol elastic

and electric dipole interactions strengthen equally with increased TLS concentration, as a result of the reduced typical distance between TLSs. However, in the first protocol, in addition to the reduced distance between TLSs, the increased strain with TLS concentration results in a decreased ratio of the electric dipolar to elastic TLS-TLS interactions. This is reflected in the temperature dependence of the sound velocity as fitted with the DOS of Eq. (4), with a smaller power μ as TLS concentration is increased [Fig. 5(a)]. However, in the mixed crystal plotted in Fig. 5(b) strain is large and independent of TLS concentration, leading to a similar and small value of μ at TLS concentrations of 4% and 7%.

V. SUMMARY

We have considered TLSs in amorphous solids for which their mutual interactions are not much smaller than the randomness in their bias energies. Such a scenario emerges naturally within the Two-TLS model, provided that electric interactions dominate over elastic interactions. Data for BK7 and coverglass [49] attest for somewhat larger electric dipolar than elastic interactions in these materials, and typical parameters for amorphous solids used in superconducting resonators suggest that stronger dominance of the electric dipolar interactions may be expected. Experiments in disordered lattices further show correspondence between the relative strength of the electric dipolar interactions and the temperature dependence of the sound velocity in agreement with our theory.

Our results suggest a microscopic origin for the power law dependence of the single-particle TLS-DOS at low energies, as found experimentally, and for the resulting anomalous exponents of the low-temperature thermal conductivity and specific heat and the temperature dependence of the acoustic velocity and dielectric constant at low-temperatures.

Energy-dependent TLS-DOS, albeit weaker, is obtained also within the dipolar gap theory of the STM [29]. A comprehensive study of the relation between the acoustic and dielectric responses in various amorphous solids could attest for the abundance of systems in which dipolar interactions dominate over elastic interactions, and for the relevance of the dipolar gap theory and the Two-TLS model in describing the low-energy properties of amorphous solids at low temperatures.

ACKNOWLEDGMENTS

SM acknowledges support from the Minerva foundation. AB and AM acknowledge partial support by the National Science Foundation (CHE-1462075). AB acknowledges the support of LINK Program of NSF and Louisiana Board of Regents and MPIPES (Dresden, Germany) Visitor Program in 2018 and 2019. MS acknowl-

edges support from the Israel Science Foundation (Grant No. 821/14 and Grant No. 2300/19).

Appendix A: Two-TLS model

While Hamiltonian (2) is standard in the theory of interacting TLSs [24], we now derive it as a low-energy effective Hamiltonian of the Two-TLS model [13]. This allows the determination of the energy scales of the TLS-TLS interactions and of the random fields, and the ratio between the two energy scales for both cases of elastic dominated and electric dominated TLS-TLS interactions.

The Two-TLS model was microscopically derived [13] and thoroughly validated [44–48] for disordered lattices which share the same universal low temperature phenomena with amorphous solids [2]. Here we assume the generalized validity of the Two-TLS model in describing TLSs in amorphous solids. Such a view point is supported by: (i) TLS-dictated low-energy properties show the same universal phenomena in disordered lattices and in amorphous solids [2], and careful experimental work suggests that universality in both groups of systems is of the same origin [60, 62, 63] (ii) The Two-TLS model derives the smallness and universality of phonon attenuation as is given by the universal dimensionless “tunneling strength” [2, 6, 7] for both disordered lattices and amorphous solids (iii) the Two-TLS model was found useful in explaining TLS pure dephasing and nonlinear absorption in superconducting qubit and microresonator circuits, not accounted for by the STM [64–66].

First considering only elastic interactions, the Two-TLS model divides TLSs into two groups, with bimodal distribution of their interaction strengths with the strain, leading to the TLS-phonon interaction Hamiltonian [13]

$$\mathcal{H}_{\text{int}} = - \sum_i \sum_{\alpha, \beta} (\eta_i \delta_{\alpha\beta} + \gamma_{w, \alpha\beta}^i \tau_i^z + \gamma_{s, \alpha\beta}^i S_i^z) \varepsilon_{\alpha\beta}^i. \quad (\text{A1})$$

Here, $\varepsilon_{\alpha\beta}^i$ is the strain tensor at TLS i , and the sum over α and β runs over the three Cartesian coordinates x , y and z . τ -TLSs possess an intrinsically small interaction with the strain, and as a result weak TLS-TLS interactions [13, 44–48]. Such TLSs constitute the predominant degrees of freedom at low energies [13, 30, 44]; their state is described by the Ising variable τ_i^z ($\tau_i^z = \pm 1$) and its weak coupling to the strain is given by the tensor $\gamma_{w, \alpha\beta}^i$. S -TLSs are described by the Ising variables S_i^z ($S_i^z = \pm 1$) and are coupled much more strongly to the strain field, with $|\gamma_{s, \alpha\beta}^i| \sim \gamma_s$, where $g \equiv \gamma_w/\gamma_s \approx 0.02$ [13, 44–48]. The first term of Eq. (A1) describes a volume energy due to the strain field which is independent on the orientation of defects, where usually $\eta_i \lesssim \gamma_s$.

The density of states (DOS) of S -TLSs strongly diminishes at low energies [13, 30, 44], and at low temperatures, for most purposes, these TLSs can be treated as frozen variables having no dynamics. They then contribute an

additional term to the energy of the same order of magnitude ($\propto \gamma_s$) as the volume term. By integrating out the phonon amplitudes, at lowest order perturbation theory, one obtains the Hamiltonian (2) as the low-energy effective Hamiltonian of the system [13], with typical random fields and interactions as are given in Eq. (9) in the main text.

Appendix B: Magnitude of the elastic and electric interactions

The parameters c_i , $c_{ij} \sim O(1)$ in Eq. (9) contain the angular dependence of the random field and the interaction. Generally, the c_{ij} parameters have a complicated dependence on the relative orientation and position of the TLSs, and can be regarded as normally distributed random variables [45]. Under this assumption one can establish a connection between the interaction strength expressed as the dimensionless parameter $P_0 \langle |\tilde{J}_{0, \text{el}}| \rangle$ for the elastic interaction and $P_0 \langle |\tilde{J}_{0, \text{dip}}| \rangle$ for the electric dipolar interaction, assuming that only terms with the transverse sound velocity v_t are significant for the elastic interaction. Here $\tilde{J}_{0, \text{el}}$ and $\tilde{J}_{0, \text{dip}}$ are interaction constants for elastic and electric interactions, respectively.

Then for the elastic interaction one can express the internal friction as $Q^{-1} = \frac{\pi}{2} P_0 \gamma_0^2 / (\rho v_t^2)$, where γ_0^2 is the average squared of the off-diagonal component of the TLS-strain interaction constant tensor, and the logarithmic slope of the temperature dependence of the sound velocity in the resonant regime as $C_{\text{el}} = P_0 \gamma_0^2 / (\rho v_t^2)$ [49]. The average absolute value of TLS-TLS interaction constant [12, 45] has been evaluated numerically assuming independent Gaussian distributions of elastic tensor components, similarly to Ref. 67, and it can be expressed as $P_0 \langle |\tilde{J}_{0, \text{el}}| \rangle \approx 1.1Q^{-1} = 1.74C_{\text{el}}$. Similar analysis for the electric dipolar interaction yields $P_0 \langle |\tilde{J}_{0, \text{dip}}| \rangle \approx 0.36 \tan \delta = 0.56C_{\text{dip}}$, where C_{dip} is the slope of the logarithmic temperature dependence of the dielectric constant. Consequently, the ratio of the two averaged interaction constants $r \equiv \langle |\tilde{J}_{0, \text{dip}}| \rangle / \langle |\tilde{J}_{0, \text{el}}| \rangle$ can be expressed as $r = 0.36 \tan \delta / (1.1Q^{-1}) = 0.56C_{\text{dip}}/1.74C_{\text{el}}$. Using the available experimental data for loss tangent and internal friction we find for SiO₂ that elastic interactions dominate ($C_{\text{el}} = 0.17 - 0.23 \cdot 10^{-3}$ [68], $Q = 3.3 \cdot 10^{-4}$ [69], yields $r = 0.3$); yet for BK7 and coverglass [49] we find dominant electric dipolar interactions (BK7: $C_{\text{dip}} = 1.51 \cdot 10^{-3}$, $C_{\text{el}} = 3.2 \cdot 10^{-4}$ yields $r = 1.51$, coverglass: $C_{\text{dip}} = 1.69 \cdot 10^{-3}$, $C_{\text{el}} = 3.6 \cdot 10^{-4}$ also yields $r = 1.51$). It would be of much interest to further investigate experimentally the magnitudes of the elastic and electric TLS-TLS interactions in amorphous solids. We further note that our estimates above neglect variations at short range of the elastic interaction and of the dielectric constant, both of which may enhance the magnitude of the electric TLS-TLS interactions in comparison to the magnitude of the elastic TLS-TLS interactions and in comparison

to the elastically dominated typical random fields.

-
- [1] C. C. Yu and A. J. Leggett, *Comments Condens. Matter Phys.* **14**, 231 (1988).
- [2] R. O. Pohl, X. Liu, and E. Thompson, *Rev. Mod. Phys.* **74**, 991 (2002).
- [3] R. C. Zeller and R. O. Pohl, *Phys. Rev. B* **4**, 2029 (1971).
- [4] S. Hunklinger and A. K. Raychaudhuri, *Prog. Low Temp. Phys.* **9**, 265 (1986).
- [5] W. A. Phillips, *Rep. Prog. Phys.* **50**, 1657 (1987).
- [6] P. W. Anderson, B. I. Halperin, and C. M. Varma, *Philos. Mag.* **25**, 1 (1972).
- [7] W. A. Phillips, *J. Low-Temp. Phys.* **7**, 351 (1972).
- [8] V. G. Karpov, M. I. Klinger, and F. N. Ignat'ev, *Sov. Phys. JETP* **57**, 439 (1983).
- [9] Y. M. Galperin, V. G. Karpov, and V. I. Kozub, *Advances in Physics* **38:6**, 669 (1989).
- [10] D. A. Parshin, *Phys. Rev. B* **49**, 9400 (1994).
- [11] A. L. Burin and Y. Kagan, *JETP* **82**, 159 (1996).
- [12] A. L. Burin, D. Natelson, D. D. Osheroff, and Y. Kagan, in *Tunneling Systems in Amorphous and Crystalline Solids*, edited by P. Esquinazi (Springer, Berlin, 1998).
- [13] M. Schechter and P. C. E. Stamp, *Phys. Rev. B* **88**, 174202 (2013).
- [14] V. Lubchenko and P. G. Wolynes, *Phys. Rev. Lett.* **87**, 195901 (2001).
- [15] V. Lubchenko, *Adv. Phys. X* **3**, 1510296 (2018).
- [16] K. Agarwal, I. Martin, M. D. Lukin and E. Demler, *Phys. Rev. B* **87** 144201 (2013).
- [17] H. M. Carruzzo and C. C. Yu, arXiv:1919.09258.
- [18] M. Schechter, P. Nalbach, and A. L. Burin, *New J. Phys.* **20**, 063048 (2018).
- [19] S. Rau, C. Enss, S. Hunklinger, P. Neu and A. Wurger, *Phys. Rev. B* **52**, 7179 (1995)
- [20] P. Strehlow, C. Enss and S. Hunklinger, *Czech. J. Phys.* **46**, 2231 (1996)
- [21] C. Enss and S. Hunklinger, *Phys. Rev. Lett.* **79**, 2831 (1997).
- [22] P. Strehlow, C. Enss and S. Hunklinger, *Phys. Rev. Lett.* **80**, 5361 (1998).
- [23] K. A. Topp, E. Thompson, and R. O. Pohl, *Phys. Rev. B* **60**, 898 (1999).
- [24] J. L. Black and B. I. Halperin, *Phys. Rev. B* **16**, 2879 (1977).
- [25] C. Enss, *Physica B* **316-317**, 12 (2002).
- [26] A. L. Efros and B. I. Shklovskii, *J. Phys. C* **8**, L49-L51 (1975).
- [27] S. D. Baranovski, B. I. Shklovskii, and A. L. Efros, *Zh. Eksp. Teor. Fiz.* **78**, 395 (1980) [Sov. Phys. JETP 51, 688 (1980)].
- [28] H. M. Carruzzo, E. R. grannan, and C. C. Yu, *Phys. Rev. B* **50**, 6685 (1994).
- [29] A.L. Burin, *J. Low Temp. Phys.* **100**, 309 (1995).
- [30] A. Churkin, I. Gabdank, A. Burin, and M. Schechter, arXiv:1307.0868.
- [31] S. T. Skacel, Ch. Kaiser, S. Wuensch, H. Rotzinger, A. Lukashenko, M. Jerger, G. Weiss, M. Siegel, and A. V. Ustinov, *Appl. Phys. Lett.* **106**, 022603 (2015).
- [32] R. B. Stephens, *Phys. Rev. B* **8**, 2896 (1973).
- [33] J. G. Lasjaunias, A. Ravex, M. Vandorpe and S. Hunklinger, *Solid State Commun.* **17**, 1045 (1975).
- [34] P. J. Selzer, D. L. Huber, D. S. Hamilton, W. M. Yen, and M. J. Weber, *Phys. Rev. Lett.* **36**, 813 (1976).
- [35] J. Hegarty, M. M. Broer, B. Golding, J. R. Simpson, and J. B. MacChesney, *Phys. Rev. Lett.* **51**, 2033 (1983).
- [36] H. P. H Thijssen, R. van den Berg, and S. Völker, *Chem. Phys. Lett.* **97**, 295 (1983).
- [37] D. L. Huber, M. M. Broer, and B. Golding, *Phys. Rev. Lett.* **52**, 2281 (1984).
- [38] R. Silbey and K. Kassner, *J. Lumin.* **36**, 283 (1987).
- [39] E. Geva and J. L. Skinner, *J. Phys. Chem. B* **101**, 8920 (1997).
- [40] J. Burnett, L. Faoro, I. Wisby, V. L. Gurtovoi, A. V. Chernykh, G. M. Mikhailov, V. A. Tulin, R. Shaikhaidarov, V. Antonov, P. J. Meeson, A. Y. Tzalenchuk, and T. Lindström, *Nat. Commun.* **5**, 4119 (2014).
- [41] L. Faoro and L. B. Ioffe, *Phys. Rev. B* **91**, 014201 (2015).
- [42] S. E. de Graaf, L. Faoro, J. Burnett, A. A. Adamyan, A. Y. Tzalenchuk, S. E. Kubatkin, T. Lindström, and A. V. Danilov *Nat. Commun.* **9**, 1143 (2018).
- [43] A. L. Burin, S. Matityahu, M. Schechter, *Phys. Rev. B* **92**, 174201 (2015).
- [44] A. Churkin, D. Barash, and M. Schechter, *Phys. Rev. B* **89**, 104202 (2014).
- [45] M. Schechter and P. C. E. Stamp, *J. Phys.: Condens. Matter* **20**, 244136 (2008).
- [46] A. Gaita-Arino and M. Schechter, *Phys. Rev. Lett.* **107**, 105504 (2011).
- [47] A. Churkin, D. Barash, and M. Schechter, *J. Phys.: Condens. Matter* **26**, 325401 (2014).
- [48] A. Gaita-Arino, V. F. Gonzalez-Albuixech, and M. Schechter, *Europhys. Lett.* **109**, 56001 (2015).
- [49] D. Natelson, D. Rosenberg, D. D. Osheroff, *Phys. Rev. Lett.* **80**, 4689 (1998).
- [50] B. Golding and J. E. Graebner, *Phys. Rev. Lett.* **37**, 852 (1976).
- [51] A. Heuer and R. J. Silbey, *Phys. Rev. B* **49**, 1441 (1994).
- [52] G. J. Grabovskij, T. Peichl, J. Lisenfeld, G. Weiss, and A. V. Ustinov, *Science* **338**, 232 (2012).
- [53] A. P. Paz, I. V. Lebedeva, I. V. Tokatly, and A. Rubio, *Phys. Rev. B* **90**, 224202 (2014).
- [54] J. M. Martinis, K. B. Cooper, R. McDermott, M. Steffen, M. Ansmann, K. D. Osborn, K. Cicak, S. Oh, D. P. Pappas, R. W. Simmonds, and C. C. Yu, *Phys. Rev. Lett.* **95**, 210503 (2005).
- [55] J. Lisenfeld, G. J. Grabovskij, C. Müller, J. H. Cole, G. Weiss, and A. V. Ustinov, *Nat. Commun.* **6**, 6182 (2015).
- [56] T. C. DuBois, M. C. Per, S. P. Russo, and J. H. Cole, *Phys. Rev. Lett.* **110**, 077002 (2013).
- [57] M. S. Khalil, S. Gladchenko, M. J. A. Stoutimore, F. C. Wellstood, A. L. Burin, K. D. Osborn, *Phys. Rev. B* **90**, 100201(R) (2014).
- [58] B. Sarabi, A. N. Ramanayaka, A. L. Burin, F. C. Wellstood, and K. D. Osborn, *Phys. Rev. Lett.* **116**, 167002 (2016).
- [59] C. Muller, J. H. Cole, and J. Lisenfeld, *Rep. Prog. Phys.* **82**, 124501 (2019).

- [60] R. O. Pohl, X. Liu, and R. S. Crandall, *Current Opin. Sol. St. Mat. Sci.* **4**, 281 (1999).
- [61] S. K. Watson *Phys. Rev. Lett.* **75**, 1965 (1995).
- [62] J. J. De Yoreo, W. Knaak, M. Meissner, and R. O. Pohl, *Phys. Rev. B* **34**, 8828 (1986).
- [63] X. Liu, P. D. Vu, R. O. Pohl, F. Schiettekatte, and S. Roorda, *Phys. Rev. Lett.* **81**, 3171 (1998).
- [64] J. Lisenfeld, A. Bilmes, S. Matityahu, S. Zanker, M. Marthaler, M. Schechter, G. Schön, A. Shnirman, G. Weiss, and A. V. Ustinov, *Sci. Rep.* **6**, 23786 (2016).
- [65] S. Matityahu, A. Shnirman, G. Schön, and M. Schechter, *Phys. Rev. B* **93**, 134208 (2016).
- [66] N. Kirsh, E. Svetitsky, A. Burin, M. Schechter, and N. Katz, *Phys. Rev. Materials* **1**, 012601 (2017).
- [67] A. L. Burin, J. M. Leveritt, Ruyters, G., C. Schötz, M. Bazrafshan, P. Fassel, M. von Schickfus, A. Fleischmann, and C. Enss, *Europhys. Lett.* **104**, 57006 (2013).
- [68] D. J. Salvino, S. Rogge, B. Tigner, and D. D. Osheroff, *Phys. Rev. Lett.* **73**, 268 (1994).
- [69] J. Classen, T. Burkert, C. Enss, and S. Hunklinger, *Phys. Rev. Lett.* **84**, 2176 (2000).